



Nanofuel Droplet Evaporation Processes

Nwabueze G. Emekwuru^{*} 

Abstract | The concern about the level of toxic emissions from the use of fossil fuels in internal combustion engines is widely held. Several alternatives have been suggested to mitigate this concern including the use of biofuels in the engines, hybrid internal combustion–electric power systems and electric propulsion systems. In the last decade there has been progress with adding nano-sized particle additives to hydrocarbon fuels with the aim of improving the thermo-physical properties. The nano-sized metallic particles increase the surface-to-volume ratio of the resultant nanofuel suspensions. Reductions in the emissions levels from the combustion of these nanofuels have been reported; these improvements derive from the reductions in ignition delay, and therefore, higher burning rates arising from increases in the evaporation rates of the fuel droplets. Thus, droplet evaporation mechanisms influence the ignition time of the droplets, and consequently the ignition delay time. Optimizing these parameters can help to reduce the emissions from the internal combustion engines. The study presented here examines the up-to-date results of work carried out by various researchers on the droplet evaporation mechanisms of nanofuel droplets. The predominant processes presented as being responsible for the enhancement of the droplet evaporation rate are that the nanoparticle additives increase the droplet fuel temperature by radiative absorption, and that at high temperature values the agglomerates of the nanoparticles heat up residuals of the liquid fuel causing fuel droplet disruptions and micro-explosions. The various parameters that affect these and other nanofuel droplet evaporation mechanisms are presented. A case is made for further studies in this area.

Keywords: Atomization, Droplet combustion, Droplet disruption, Droplet dry-out, Droplet evaporation, Droplet radiative absorption, Energetic fuels, Micro-explosion, Nano-sized particles, Nanofluids, Nanofuels

1 Introduction

Fuel droplet evaporation is of interest in many applications. Spark ignition and compression ignition engines and gas turbine systems in which liquid fuels are combusted are important examples. These internal combustion engines contribute to the global greenhouse gas emissions and the concerns about this have led to the development of biofuels, hybrid internal

combustion–electric powerplants and pure electric powerplants.

In internal combustion engines that use liquid fuels, the fuel droplet evaporation rates influence the ignition temperature, therefore the ignition time of the droplets, and thus, the ignition delay. Optimizing these parameters can improve the efficiency of the engine, thus affecting the emissions and fuel consumption levels.

¹ School of Mechanical, Aerospace and Automotive Engineering, Coventry University, Coventry, UK.
*ab9992@coventry.ac.uk

Recent advances in nanotechnology have included the ability to manufacture energetic nanoparticles (NPs) of specific properties. NPs are usually metallic particles of nano size (10–100 nm range) with high rates of energy release^{4, 19, 23, 32} and volumetric heat of oxidation²⁴.

The addition of NPs to solid fuels has been a subject for investigators for decades^{7, 9, 24, 30, 33}. Results from these investigations indicated that the addition of these NPs to the solid fuels can decrease the ignition delay²⁴ due to the increase in the surface-to-volume ratio^{15, 28}. As a consequence of the rapid temperature gradients present in the thin oxide layers of the NPs, they can also ignite below the bulk-metal melting point^{26, 31, 34}. In the last two decades, studies have shown that the addition of the NPs to fluids can improve the thermo-physical properties of the fluids, including the rate of evaporation⁵. Thus, it was inevitable that the principle would be applied to liquid fuels, with some of the early studies indicating that the addition of Al or Al₂O₃ NPs to diesel reduced the evaporation time, and hence, the ignition times compared to pure diesel fuel droplets⁴³, and similar effects were also observed for Al NPs added to ethanol compared to pure ethanol¹.

Since then studies have been conducted on the fundamental aspects and applications of nanofuels. For instance, Miglani and Basu²⁷ observed that the secondary atomization behaviour of burning nanofuels consisted of disruptive modes. These disruptive modes were characterised by the expulsion of internally nucleated bubbles and this process enables the transportation of the NPs from the primary nanofuel droplet to the flame and this leads to flame disruption. The intensity of these disruptive modes increased by increasing the NP concentration in the nanofuel. Tanvir and Qiao⁴¹ showed that increasing the NP concentration can increase the particle aggregation intensity in the nanofuel solution, which in turn affects the burning rates of the nanofuel droplets. Kannaiyan and Sadr²⁰ examined the effects of NP on aviation jet fuel sprays and observed increases in the nanofuel viscosity and density with increase in NP concentration. Asibor et al.² have predicted the effects of NP concentrations on aviation fuel at ambient conditions using existing correlations for hydrocarbon fuels.

The review reports present in the literature with regard to nanofuels have mostly evaluated the work on the application of nanofuels to internal combustion engines (ICEs). Studies by Khond and Kriplani²², Shaafi et al.³⁸ and Saxena et al.³⁵ all examined the performance and emission characteristics of ICEs running on nanofuels. The

review reports by Basu and Miglani³ and Karmakar et al.²¹ are the only recent ones examining studies related to nanofuel combustion and heat transfer characteristics. The author is unaware of any review report specifically examining nanofuel droplet evaporation phenomena. The motivation for this study is, thus, to examine and present the current understanding of the evaporation characteristics of nanofuel droplets and to suggest areas for further studies. The autoignition and combustion processes have not been considered.

The next two sections give a background to the evaporation phases of fuel droplets and the studies outlining the evaporation phases observed for nanofuel droplets. Section 4 presents the current mechanisms that have been proposed as to how the nanofuel droplet evaporation occurs. The results from studies evaluating the behaviour of evaporating nanofuel droplets with respect to the D^2 law are presented next. In Section 6, the effects of the nanoparticle type and concentration are evaluated. The studies that have evaluated the effect of the surfactants on the nanofuel droplet evaporation are considered in the subsequent section. Other factors that influence the vaporization process are analysed in Sect. 8. The possible areas for further studies are presented in Sect. 9. The report is concluded in the last section.

2 Evaporation Phases of Fuel Droplets

The phases of liquid fuel droplet evaporation are well known. Effective atomization increases the surface area of a liquid sheet of fuel by disintegrating the sheet into large numbers of fuel droplets, thereby increasing the mixing and evaporation rates leading to a lower ignition point, improved fuel droplet burning and consequently lower fuel consumption and pollutant emissions levels²⁵. The increased surface area during the atomization process increases the rate of heat transfer from the surrounding gas to the fuel droplets. As the rate of heat transfer increases, the temperature of the fuel droplet increases as its mass simultaneously decreases due to vaporization to the surrounding gas. At some point during the process, the fuel droplet–gas mixture reaches its self-ignition temperature or can be ignited by several means²⁵. The process can be presented as a series of simplified processes as prescribed by Faeth⁸ and referring to the representation of the variation of the fuel droplet size with evaporation time in Fig. 1 as: (1) if a pure fuel droplet is exposed to a high-temperature gaseous environment, there is initially a low concentration of fuel vapour on the liquid surface, and

Nanofuels: are an exciting new class of fuels that utilize nano-sized particle additives to the base fuel and have the potential to reduce the emissions from internal combustion engines.

This report presents and examines the up-to-date results of work carried out by various researchers on the droplet evaporation mechanisms of nanofuel droplets.

The predominant processes presented as being responsible for the enhancement of the droplet evaporation rate are that the nanoparticle additives increase the droplet fuel temperature by radiative absorption, and that at high temperature values the agglomerates of the nanoparticles heat up residuals of the liquid fuel causing fuel droplet disruptions and micro-explosions.

It is hoped that scholars working on the fundamentals and applications of droplet and atomization processes and engineers designing internal combustion systems using alternative fuels, will find the report useful.

minimal transfer of mass from the droplet (Phase I on Fig. 1). This is the heat-up phase of the fuel droplet evaporation process. (a) The gradient of the slope of the droplet size versus the evaporation time graph is small. (b) The fuel droplet temperature is uneven, with the surface of the droplet being hotter than the centre of the droplet. (c) Most of the heat being gained by the droplet is used to raise its temperature and this leads to part of it being used to feed the heat of vaporization of the fuel droplet and the increasing fuel vapour on the surface of the droplet, reducing the rate of heat transfer from the gaseous environment to the fuel droplet, thus the fuel droplet temperature becomes more uniform. (2) Eventually the fuel droplet settles at its wet-bulb temperature at the point when all the heat gained by the droplet is used to feed its heat of vaporization. This is the Phase II on Fig. 1. This is the steady-state phase of the fuel droplet evaporation process.

The relative sizes of the heat-up and steady-state phases in Fig. 1 depend on the operating conditions and volatility of the fuels being studied. However, Godsave¹⁴ showed that, considering just the steady-state phase in Fig. 1, with $\lambda_{st} = \lambda$, then the variation of square of the fuel droplet size with evaporation time can be represented by a straight line as:

$$D_0^2 - D^2 = \lambda t. \quad (1)$$

This relationship, which has been useful in the analyses of fuel droplet evaporation processes, is known as the D^2 law of droplet evaporation. D_0 is the initial droplet diameter and λ is the evaporation constant

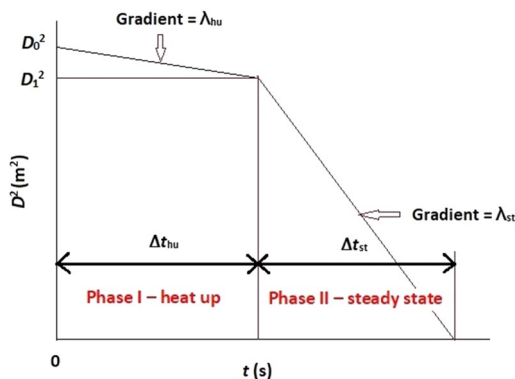


Figure 1: A representation of the variation of fuel droplet sizes with evaporation time, showing the heat-up (hu) and steady-state (st) phases. (Adopted from [14]).

3 Evaporation Phases of Nanofuel Droplets

A summary of the nanofuel droplet evaporation studies carried out by researchers is presented in Table 1. The table also includes the experimental conditions for the studies. The present section outlines the distinct phases that have been discerned from the studies of the evaporation processes of nanofuel droplets.

Researchers have identified, broadly, three phases (see Table 2) during the nanofuel droplet evaporation mechanism; in addition to the first two phases presented in Sect. 2, a third phase, the droplet ‘dry-out’ phase, typified by the presence of some residuals of the NPs after the near complete evaporation of the base fuel liquid at the end of the steady-state phase, or a droplet disruption/micro-explosion stage, at temperature values much higher than the boiling temperature of the base fuel. The duration of any of these phases varies widely depending on the operating conditions prevailing at the time.

3.1 Evaporation Phases at Natural Convection or Weak Forced Convection Conditions

Gan and Qiao¹⁰, during their studies of Al–ethanol and Al–*n*-decane nanofuels under natural convection and weak forced convection droplet evaporation conditions, observed three distinct regions (Fig. 2): (1) under heated nitrogen streams, there was weak forced convection leading to a slight increase in the droplet temperature after a very short (about 3 s) heat-up phase. The droplet size reduction was only slight. This is similar to the heat-up phase in Fig. 1. (2) After this period under the heated nitrogen streams, the weak forced convection is almost constant with time, with a very small rise in the temperature of the droplet over this period as the droplet size falls linearly with time in a steady-state evaporation phase. This region is akin to the steady-state region in Fig. 1. (3) In the third region, the dry-out phase, the fuel liquid in the nanofuel mixture completely dries out, leaving behind nanoparticle agglomerates of about 100 μm. Gan and Qiao¹¹ also observed these three-phase phenomena during their Al₂O₃–ethanol nanofuel droplet evaporation studies, though in their CNP–ethanol and MWCNT–ethanol cases¹² the dry-out phase was not explicitly mentioned.

Table 1: Evaporation of fuel droplets with nanoparticle additives reported in the literature currently.

Authors	Base fuel and type of surfactant (S)	Type of nanoparticle, size (nm) and particle loading rate (PLR)	Operating conditions and evaporation characteristics studied
Gan and Qiao ¹⁰	<i>n</i> -Decane, ethanol (S) Sorbitan oleate 0.5 wt%	Aluminum (mean diameter 80 nm) 1 wt%	Evaporation under natural convection at room temperature, under weak forced convection at up to 227 °C
Gan and Qiao ¹¹	Ethanol No surfactant (due to a previous study ³⁹ excluding the need for this)	Aluminum (mean diameter 80 nm) 0.1, 0.5, 5 wt% Aluminum oxide—Al ₂ O ₃ (mean diameter 25 nm) 0.1, 0.5, 5 wt%	Evaporation under different radiation levels, characterised by the light intensity of a mercury lamp, from 75 to 175 W in increments of 25 W
Gan and Qiao ¹²	Ethanol No surfactant (as in ¹¹)	Carbon nanoparticles (6 nm) 0.1 wt% Multiwalled carbon nanotubes. 0.1 wt%	Evaporation under different radiation levels, characterised by the light intensity of a mercury lamp, from 75 to 175 W in increments of 25 W
Javed et al. ¹⁶	Kerosene (S) Oleic acid (diameter 100 µm) 0.25 wt% 0.5 wt%	Aluminum (70 nm)	Ambient temperature 400–800 °C Ambient pressure 0.1 MPa
Javed et al. ¹⁷	Heptane (S) Sorbitan trioleate (span 85). 0.5, 1.0, 2.5, 5 wt%	Aluminum (70 nm) 0.5, 2.5, 5 wt%	Ambient temperature 100–600 °C Ambient pressure 0.1 MPa
Javed et al. ¹⁸	Kerosene (S) Oleic acid (diameter 100 µm) 0.25 wt% 0.5 wt%	Aluminum (70 nm) 2.5, 5.0, 7.0 wt%	Ambient temperature 400–800 °C. Ambient pressure 0.1 MPa
Gerken et al. ¹³	Ethanol No surfactant	Aluminum (40–60 nm diameter) 0, 0.1, 0.27, 1, 3.06 wt%	Ambient temperature 24 °C Atmospheric pressure Relative humidity 35–45%
Yoon and Baek ⁴⁴	Kerosene (S) Oleic acid (diameter 100 µm) 0.25 wt% 0.5 wt%	Aluminum (70 nm) 0.1, 1.0 wt%	Ambient temperature 300–700 °C Ambient pressure 0.1, 2.5 MPa
Tanvir et al. ⁴²	Ethanol No surfactant	Graphite (50 nm mean diameter) 1, 3, 5 wt%	2.3 µm diode laser of 2 mW constant power used as the infrared radiation source

Table 2: Nanofuel droplet evaporation phases.

Operating conditions	Phase I	Phase II	Phase III
Natural evaporation Weak forced evaporation Gan and Qiao ^{10, 11}	Heat-up phase	Steady-state phase	Droplet dry-out phase
High ambient temperature above boiling point of base fuel Javed et al. ^{16–18}			Droplet distortion/micro-explosion phase
High ambient temperature above boiling point of base fuel. Javed et al. ¹⁷ . For the case of the addition of a surfactant to the base fuel but without the NP additive			Thermal decomposition of the surfactant Droplet distortion and fragmentation

3.2 Evaporation Phases at High Ambient Temperature Conditions

Javed et al.^{16–18} carried out a series of experiments to study the mechanisms of nanofuel droplets at

temperature values much higher than the boiling temperature of the base fuel and the melting point of the metallic nanoparticle additive. In Javed et al.¹⁶, they investigated the droplet

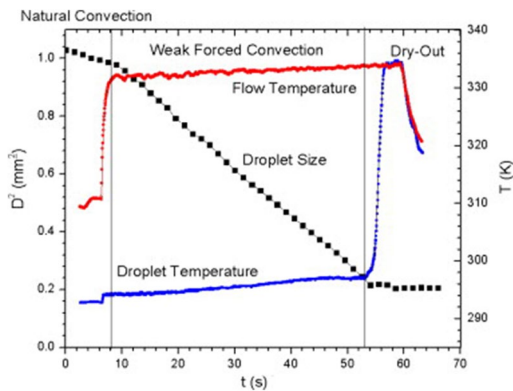


Figure 2: A representation of the variation of nanofuel droplet sizes and nanofuel droplet temperature with evaporation time, showing the heat-up (2–8 s), steady-state (8–53 s) and dry-out phases (53–62 s), for Al–ethanol nanofuel (2.5 wt%)¹⁰. Reprinted from Gan et al.¹⁰, with permission from Elsevier.

evaporation mechanisms of Al–kerosene nanofuel. To stabilise the solution, oleic acid was used as the surfactant, and a droplet-evaporating range of 400–800 °C was investigated. A number of phenomena were observed in this study: (1) the presence of a heat-up phase as presented in Fig. 1. (2) The presence of a steady-state phase. (3) A droplet distortion/micro-explosion phase. This third phase occurred at the 700–800 °C range (see Table 3). Compared with the results from the 400 to 600 °C values (Fig. 3a), the observations at the high temperature values (700–800 °C) shown in Fig. 3b indicate more volatile conditions. For all the nanoparticle concentration cases, the heat-up periods are shorter, the evaporation rates were shortened and the droplet lifetimes were shorter compared to pure kerosene droplets. The more interesting observations at these conditions were the onset of bubble formation and micro-explosions. These were a consequence of the temperature values at these conditions being higher than the boiling point of the kerosene fuel. Thus, at the onset of the heat-up period, the nanoparticles on the surface of the droplets and inside the droplets provided multiple nucleation sites that generated superheated vapours, which might have led to the droplet fragmentation also witnessed at this stage of the droplet evaporation process. However, at the later stage of the steady-state evaporation phase, most of the fuel droplets would have evaporated and agglomerates of the nanoparticles are left behind on the surface of the remaining fuel liquid. These agglomerates are exposed to the high temperature values present at this phase and

are heated up. These, in turn, heat up the remaining fuel liquid, rupturing the droplets in a series of micro-explosions. This sequence is shown in the photographs presented in Fig. 4. The nanofuel droplet rupture can be seen at $t = 1.23$ s for an Al NP concentration of 0.5 wt% (Fig. 4a) and at $t = 1.26$ s for an Al NP concentration of 1.0 wt% (Fig. 4b). Thus, the temperature of the surrounding medium in which the nanofuel droplet is laden profoundly affects the rate of evaporation and the thermo-physics especially at temperatures much higher than the boiling temperature of the base fuel and the melting temperature of the metallic nanoparticle. Similar observations were reported by Javed et al.¹⁷ for Al–heptane nanofuel droplet studies with sorbitan trioleate as the surfactant at 100–600 °C. An interesting aspect of this study was that it presented results that indicated that, even for the case of the addition of just the surfactant to the base fuel (without the NP additive), at the high temperature values, there is a thermal decomposition phase after the steady-state phase in which the surfactant residues can cause droplet distortion and fragmentation.

4 Evaporation Mechanisms of Nanofuel Droplets

This section presents the proposals made by various scholars as to how the mechanisms of nanofuel droplet evaporation occur. These proposals are supported by experimental observations and have been summarized in Table 4.

4.1 The Radiative Process Concept

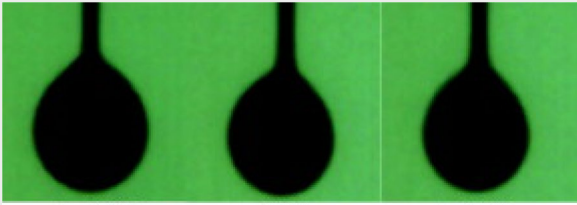
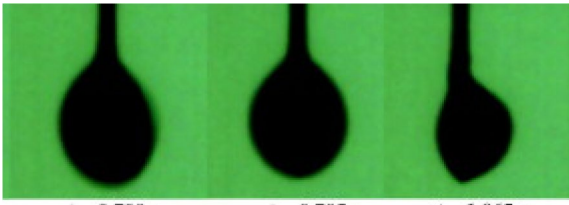
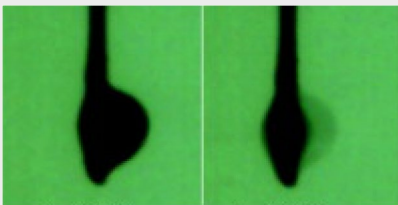
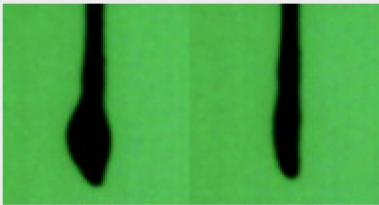
The evaporation rate of a nanofuel droplet is enhanced due to the nanofuel droplet temperature being increased by the radiative absorption properties of the metallic NP additive^{11, 12}. This decreases the heat-up period of a nanofuel droplet compared to that of a base fuel droplet.

4.2 The Latent Heat of Vaporization Concept

The addition of NPs increases the evaporation rate by reducing the latent heat of vaporization of the nanofuel solution⁴⁴. From Eq. (1), it can be shown²⁵ that the evaporation constant λ can be evaluated as a function of the thermo-physical properties of the fuel and the gaseous surroundings as:

$$\lambda = \frac{8kIn(1+B)}{C_p\rho}. \quad (2)$$

Table 3: Example of a nanofuel droplet undergoing the evaporation phases. Reprinted from Javed et al. (2014), with permission from Elsevier.

Operating conditions	High ambient temperature above boiling point of base fuel. Sequential photographs of vaporization of Al-kerosene nanofuel droplets with 2.5 wt% Al NPs coated with 1.25% oleic acid) at 800 °C Javed et al. ¹⁸
Phase I Heat-up phase	 <p data-bbox="874 583 1463 659">The heat-up phase. At $t=0.695$ s there is a slight increase in the nanofuel droplet diameter due to vapour formation on the droplet surface</p>
Phase II Steady-state phase	 <p data-bbox="874 898 1463 974">The steady-state phase. The nanofuel droplet diameter reduces as the vapour escapes the droplet [$t=0.700$ s] and the nanofuel droplet vaporizes linearly in droplet size</p>
Phase III Droplet distortion/micro-explosion phase	 <p data-bbox="874 1213 1463 1268">Internal bubble formation inside the droplet [$t=1.210$ s] occurs and the droplet ruptures [$t=1.215$ s]</p>
Droplet dry-out phase	 <p data-bbox="874 1507 1463 1545">The droplet dries out leaving minute quantities of NP residuals</p>

B in Eq. (2) is a function of the latent heat of vaporization, L , thus:

$$B = \frac{C_p (T_\infty - T_s)}{L} \tag{3}$$

Therefore:

$$\lambda \propto B \propto \frac{1}{L} \tag{4}$$

This concept was first attributed to the enhancement of the evaporation rate of deionized water laden with NP additives⁵.

4.3 The Droplet Disruption/ Micro-Explosion Concept

At high ambient temperatures much higher than the boiling point of the base fuel, the nanofuel droplet evaporation is enhanced by the droplet disruptions and micro-explosions caused by the

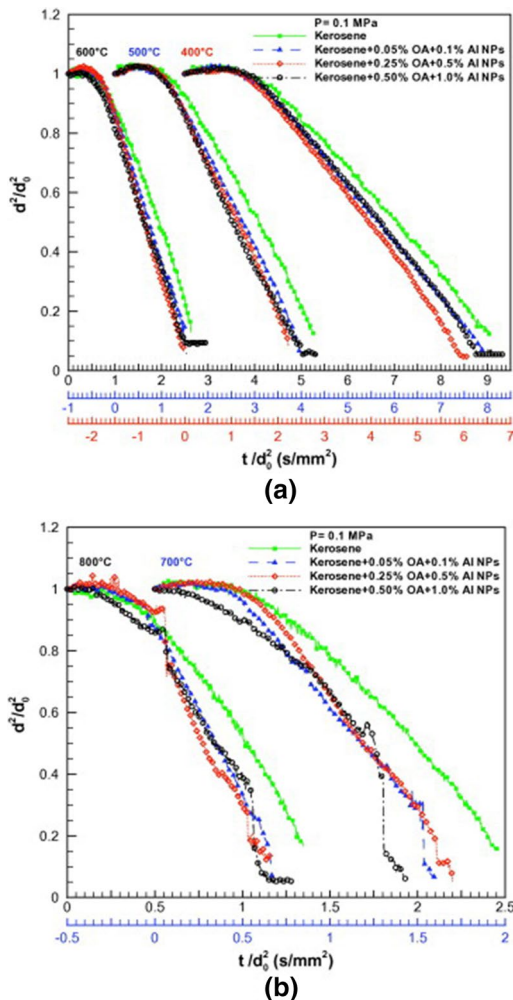


Figure 3: A representation of the variation of nanofuel droplet sizes with evaporation time, for Al–kerosene nanofuel (0.1, 0.5, 1.0 wt%), with oleic acid (OA) surfactant, at ambient temperature values of **a** 400, 500 and 600 °C, and **b** 700 and 800 °C. The colour of the x-axes scales on the graphs are for the plots of the temperature values of corresponding colour¹⁶. Reprinted from Javed et al.¹⁶, with permission from Elsevier.

heating of the NP agglomerates left behind after the initial (almost) complete evaporation of the base fuel^{17, 18}.

5 Evaporation Mechanisms of Nanofuel Droplets and the D^2 Law

Many of the studies of the evaporation mechanism of nanofuel droplets have tried to ascertain if the evaporation rates of the droplets fit the D^2 law of Godsave¹⁴. Gan and Qiao¹⁰ highlighted for the first time, a deviation from the D^2 law (Eq. 1)

for some instances of nanofuel droplet evaporation. The steady-state evaporation trends for the base fuels (*n*-decane and ethanol) followed the D^2 law under all the test conditions. For the aluminum-laden ethanol fuels, the D^2 law was observed for the weak forced convection conditions but not under the natural convection conditions (Fig. 5). For the aluminum-laden *n*-decane fuels, the D^2 law is valid for fuel droplet evaporation trends under weak forced convection conditions at elevated temperature values, but not so under ambient conditions (300 K) or under natural convection conditions (Fig. 6). The trends indicated that the deviations from the D^2 law increased with increasing nanoparticle concentration levels, for base fluids with higher boiling points, and for instances where there were long droplet lifetimes. The authors were of the opinion that these deviations occurred due to the nanoparticle aggregation inside the vaporizing fuel droplets. Javed et al.¹⁶ observed the D^2 law for the base fuel with the surfactants, and for the Al–kerosene nanofuel with oleic acid surfactants up to 600 °C. At between 100 and 300 °C for Al–heptane¹⁷, and for Al–ethanol at 24 °C¹³, the D^2 law was also observed. However, for high (600–800 °C) temperature conditions where droplet distortion and micro-explosions are prominent¹⁸, the heat-up and steady-state phases are much shorter; with the droplet distortion and micro-explosion phase having more significance, it is not possible to apply the D^2 law. A comparison of Fig. 3a with b highlights this.

6 Effect of the Type of Nanoparticle Additive

In this section, details of the effects of the NP type and PLR on the characteristics of nanofuel droplet evaporation are discussed.

6.1 Effect of the Nanoparticle Type

The studies conducted so far examining the effect of the NP type on the evaporation of nanofuel droplets have been carried out in the context of the radiative properties of the NPs (see Sect. 4.1). Gan and Qiao¹¹ compared the evaporation rates of Al–ethanol and Al₂O₃–ethanol nanofuel droplets and found the latter to have a lower rate of evaporation compared to the former. A similar study was also reported later¹² comparing Al–ethanol, CNP–ethanol and MWCNT–ethanol nanofuel droplets, and it was observed that the droplet evaporation rates increased compared to

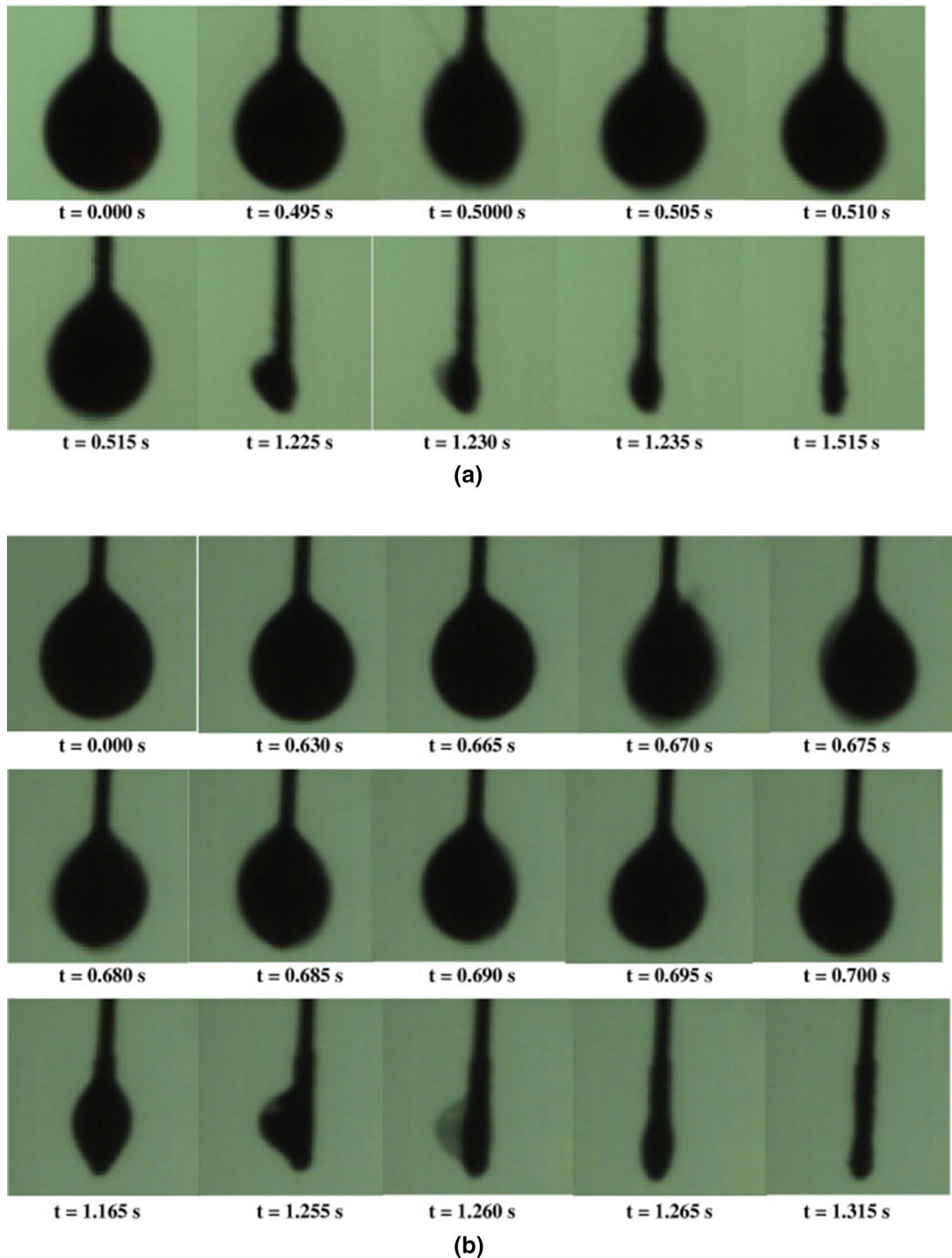


Figure 4: Sequential photographs of vaporization of Al-kerosene nanofuel droplets **a** with 0.5 wt% Al NPs at 800 °C, **b** with 1.0 wt% Al NPs at 800 °C¹⁰. Reprinted from Javed et al.¹⁰, with permission from Elsevier.

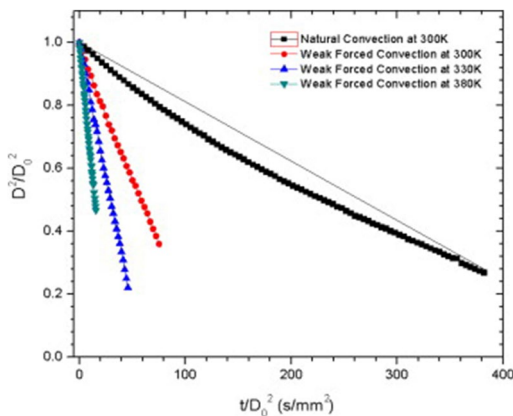
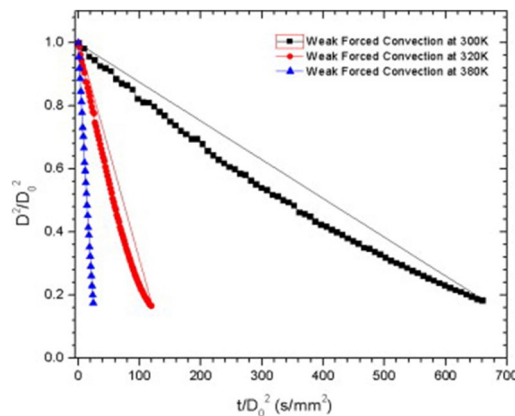
the pure ethanol fuel droplets in that order. In both studies, the authors posited that NPs which can absorb more radiative energy, when laden in fuels, result in nanofuels with higher evaporation rates compared to the base fuels.

6.2 Effect of the Nanoparticle Loading Rate on Nanofuel Evaporation

Table 5 gives a summary of examples of studies showing the competing factors that affect the effects of the PLR on the nanofuel droplet evaporation rate.

Table 4: Proposed mechanisms, supported by empirical observations, by which nanoparticles enhance the droplet evaporation rates of base fuels.

Mechanism	Details
Radiative process Gan and Qiao ^{11, 12}	NP additive has radiative absorption properties, That increase the temperature of the NP-laden base fuel droplet, That leads to the increase of the evaporation rate of the NP-laden fuel droplet.
Latent heat of vaporization process Yoon and Baek ⁴⁴	NP additive in nanofuel solution reduces the latent heat of vaporization of the solution. This leads to the increase of the evaporation rate of the NP-laden fuel droplet.
Droplet disruption/micro-explosion process Javed et al. ^{17, 18}	Agglomerates of the NP additives are left behind after the evaporation of most of the base fuel after the steady-state phase. At elevated operating temperature conditions, these NP agglomerates are heated up, They in turn heat up the remaining base fuel liquid leading to droplet disruption and micro-explosions.

**Figure 5:** A representation of the variation of nanofuel droplet sizes with evaporation time, for Al-ethanol nanofuel, under different ambient conditions, at 2.5 wt% Al NP¹⁰. Reprinted from Gan et al.¹⁰, with permission from Elsevier.**Figure 6:** A representation of the variation of nanofuel droplet sizes with evaporation time, for Al-*n*-decane nanofuel, under different ambient conditions, at 2.5 wt% Al NP¹⁰. Reprinted from Gan et al.¹⁰, with permission from Elsevier.

6.2.1 Effect on the Evaporation Rate

Gan and Qiao¹¹ investigated the effects of different concentrations of aluminum and aluminum oxide nanoparticles (0.1, 0.5, 5 wt%) of mean diameter values of 80 and 25 nm, respectively, as additives to ethanol fuel under constant radiative intensity conditions. The results from the experiments indicated that the Al-ethanol nanofuel droplet evaporation rates were enhanced for all the cases studied compared to the base ethanol fuel droplet. As the nanoparticle concentration increases, the radiative energy absorption increases as more nanoparticles become active in the radiative absorption and scattering processes. Thus, the Al-ethanol suspension with 0.5 wt% concentration, has a higher rate of droplet

evaporation compared to that with 0.1 wt% concentration. However, at high concentration values (here 5 wt%), the effects of the aggregation of the nanoparticles, which inhibit evaporation, are stronger than the radiative absorption effects. Thus, the rate of nanofuel droplet evaporation reduces compared to the lower nanoparticle concentration levels but still higher than that for the base fuel. For the cases of the Al₂O₃-ethanol nanofuels, however, the rate of droplet evaporation increase compared to the base fuel is not as marked as in the Al-ethanol nanofuel cases. In fact, at a concentration of 5 wt% the evaporation rate decreases compared to the base ethanol fuel. The authors suggest that since Al₂O₃ nanoparticles have a lower radiative energy absorption

Table 5: The effects of nanoparticle loading rate on the nanofuel evaporation rate. These are entirely dependent on the relative strengths of the competing factors in the process. A number of examples are given below to highlight these

Study details	Competing factors		Optimum PLR for the study with details
	(1)	(2)	
Al-ethanol nanofuel PLR 0.1, 0.5, 5 wt% Gan and Qiao ¹¹	Radiative energy absorption by the NPs	Formation of NP aggregates	Optimum PLR: 0.5 wt% Below 5 wt% (1)>(2) Therefore, evaporation rate increases.
Al ₂ O ₃ -ethanol nanofuel PLR 0.1, 0.5, 5 wt% Gan and Qiao ¹¹			From 5 wt% (2)>(1) Therefore, evaporation rate decreases.
Al-heptane nanofuel PLR 0.5, 2.5, 5 wt% Javed et al. ¹⁷	Operating ambient temperature of 400–600 °C much higher than the boiling point of the base fuel		Optimum PLR: 2.5 wt% Below 400 °C (2)>(1) Therefore, evaporation rate decreases. From 400 to 600 °C (1)>(2) Therefore, evaporation rate increases.
Al-ethanol nanofuel PLR 0.1, 0.27, 1, 3.06 wt% Gerken et al. ¹³	Increase in surface area available for heat transfer		For all the PLR values examined (2)>(1) Therefore, evaporation rate decreases.

compared to Al nanoparticles, they have less impact in improving the rate of evaporation of the nanofuel due to radiation energy absorption by the nanoparticles. This difference in the radiative energy absorption effect of the nanoparticles can also be seen in the droplet temperature–time plot in Fig. 7. It can be seen from the steady-state evaporation stage that the Al-ethanol nanofuel droplets have a temperature of about 19 °C compared to about 15 °C for the base ethanol fuel droplet. However, the Al₂O₃-ethanol nanofuel droplets do not show a marked increase compared to the base fuel. Javed et al.¹⁷ investigated the droplet evaporation mechanisms of Al-heptane nanofuel, with 0.5, 2.5, and 5 wt% PLR, in a similar manner to their work in Javed et al.¹⁶ at 100–600 °C. At below 400 °C, the Al-heptane nanofuel droplets exhibited a lower rate of evaporation. Below these temperature values, the aluminum nanoparticles form agglomerates which form a shell which inhibit the nanofuel evaporation. Conversely, above 400 °C the surfactants are mostly decomposed, and the agglomerates formed by the nanoparticles are small with the shells formed over the droplets porous, therefore the evaporation rates are increased. At lower

temperature values, an increase in the nanoparticle concentration values reduces the droplet evaporation rates whereas at the higher temperature values the reverse is the case. An optimum concentration value of 2.5 wt% was observed.

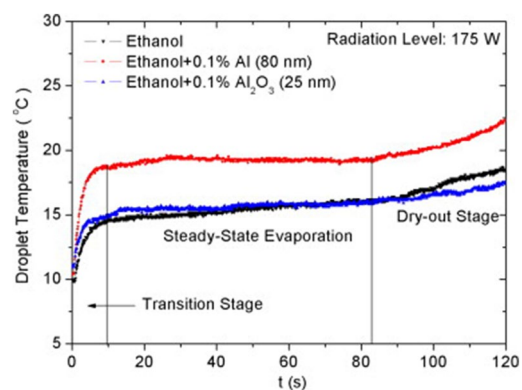


Figure 7: A representation of the variation of nanofuel droplet temperature with evaporation time, showing the heat-up ('transition stage'), steady-state and dry-out phases, for base ethanol fuel, Al-ethanol nanofuel and Al₂O₃-ethanol nanofuel¹¹. Reprinted from Gan et al.¹¹, with permission from Elsevier.

Gerken et al.¹³ varied the PLR of Al nanoparticles (1–3%) in an Al–ethanol nanofuel study and observed that the evaporation rate fell by 15% relative to the evaporation rate of pure ethanol at ambient conditions of 24 °C and relative humidity of 35–45%.

6.2.2 Effect on Droplet Distortions and Micro-Explosions

The micro-explosion phenomena during the nanofuel droplet evaporation at high temperature conditions were studied by Javed et al.¹⁸. Aluminum nanoparticles were dispersed in kerosene, with oleic acid used as the surfactant. The effects

of the concentration (2.5, 5.0, and 7.0 wt%) of the nanoparticles on the droplet distortions and micro-explosion characteristics were investigated at 400–800 °C. For the dense (5.0, and 7.0 wt% PLR) Al–kerosene nanofuel solutions, the evaporation rate is increased compared to the base kerosene fuel. Al–kerosene nanofuel droplets with 2.5 wt% PLR at 400–500 °C (Fig. 8a) showed no bubble formation and no droplet micro-explosions occurred. In contrast, the 5.0 wt% and 7.0 wt% PLR suspensions presented bubble formation and rupture at the end of the droplet lifetime. This was attributed to the accumulation of nanoparticle shells at the droplet surface that are at temperature values above that of the boiling point of kerosene, which led to nucleation sites to form inside the droplet, causing gasification of the surrounding liquid, build-up of pressure and eventually fragmentation of the droplet. Observations at the 600–800 °C (Fig. 8b) range indicated that, for all the nanoparticle concentration levels, bubble formations and micro-explosions were observed. Micro-explosions are important in the evaporation process of nanofuels because they could lead to smaller droplets which in turn enhance the combustion process. With high nanoparticle concentration levels, the micro-explosions were more intense and this also increased at the high temperature values. At these high-temperature conditions, the micro-explosions occurred with or without prior droplet expansion. These micro-explosions were not present in the cases for the pure kerosene fuel, therefore, they can be attributable to the nanoparticle additives.

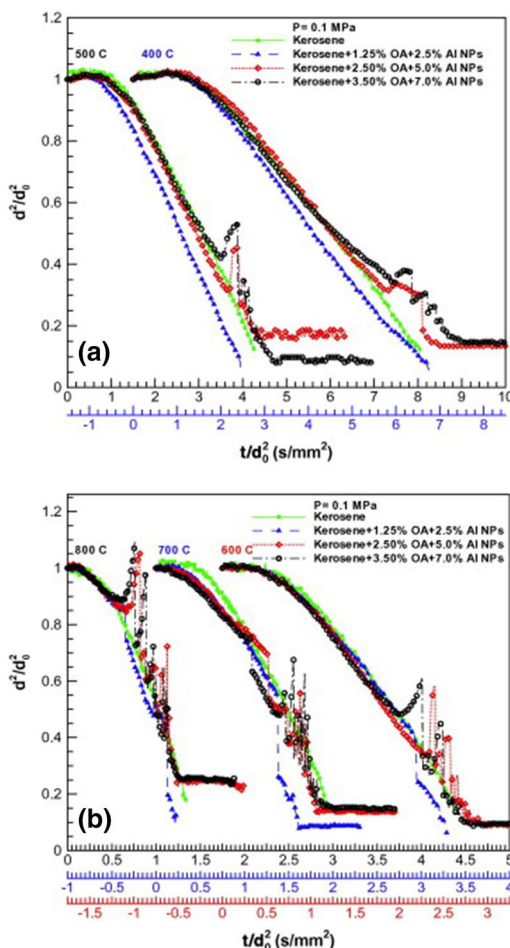


Figure 8: A representation of the variation of nanofuel droplet sizes with evaporation time, for Al–kerosene nanofuel (2.5, 5.0, 7.0 wt%), with oleic acid (OA) surfactant, at ambient temperature values of **a** 400, and 500 °C, and **b** 600, 700 and 800 °C. The colour of the x-axes scales on the graphs are for the plots of the temperature values of corresponding colour¹⁸. Reprinted from Javed et al.¹⁸, with permission from Elsevier.

6.3 Effect of the Nanoparticle Agglomerates on the Evaporation of Nanofuels

This section is closely related to Sect. 6.2. When nanofuel droplets are subjected to high-temperature gaseous conditions, the base fuel evaporates, leaving behind residuals or agglomerates of the constituent nanoparticles^{10, 16–18}. This is because the boiling points of the base fuels are usually considerably lower than the melting points of the metallic nanoparticles. For instance, kerosene has a boiling point of about 543 K and Al NP a melting point of 933 K¹⁸. Thus, when subjected to heating at temperatures closer to the evaporation temperature of kerosene, an Al–kerosene nanofuel droplet will undergo an almost complete evaporation of the base fuel of kerosene, but with agglomerates of the Al NPs left behind. This phenomenon affects the evaporation mechanisms

of nanofuel droplets, as already mentioned in Sects. 4, 5 and 6. The effects depend on the operating conditions at which the nanofuel droplet is exposed, and the PLR of the nanoparticles in the nanofuel. At operating temperature conditions well below the melting point of the NP, the NP agglomerates' effects on the evaporation mechanism of the nanofuel have been shown to depend on the radiative properties of the constituent NP and the PLR. Nanofuel droplets with NPs of poor radiative properties can exhibit evaporation rates lower than those of the base fuel at certain PLRs¹¹. For nanofuel droplets with NPs having good radiative properties, there are also threshold PLR conditions at which the rate of droplet evaporation would start to decrease^{11, 42}. This is because the rate of accumulation of the NP agglomerates on the surface of the droplets increases with the PLR and these start to reduce the radiative heating effects on the nanofuel droplets. However, at operating temperatures above the boiling point of the base fuel, the presence of the NP agglomerates profoundly change the nanofuel droplet evaporation mechanisms. In the first instance, at the start of the heat-up period, the NP inside and on the surface of the droplets provide multiple nucleation points that generate superheated vapours that lead to nanofuel droplet disruption and fragmentation. Secondly, at the late stage of the steady-state evaporation period, the NP agglomerates present after the evaporation of most of the base fuel heat up the remaining fuel liquid leading to a sequence of micro-explosions. The intensity of these processes increases with an increase in the PLR. Tables 4 and 5 summarize some of these mechanisms. Javed et al.^{16–18} also present videos depicting these events. The presence of NP agglomerates also contributes to the deviation of the nanofuel droplet evaporation rate from the D^2 law either by accumulating on the surface of the nanofuel droplets¹⁰ or by causing the phenomenon of droplet micro-explosions¹⁸.

7 Effect of the Surfactant on Nanofuel Evaporation

Javed et al.¹⁶ investigated the effect of using oleic acid as a surfactant, in 0.25 and 0.5 wt% concentration values, on the droplet evaporation mechanisms of kerosene droplets at 400–800 °C. The evaporation rates of kerosene laden with oleic acid surfactants exhibited the D^2 law as did the unladen kerosene droplets. With an increase in concentration of the oleic acid surfactant in the kerosene fuel droplet at a temperature range of 400–500 °C, a monolayer of the oleic acid is

formed on the kerosene droplet, thereby extending the evaporation time and hence reducing the rate. At higher temperature values of up to 800 °C, there were droplet distortions during the heat-up phase due to the entrapment of highly volatile components and the droplet heating-up period subsequently increased.

8 Effect of Other Operating Conditions

The operating conditions under which the nanofuel droplet is evaporating affects the competing mechanisms that affect the droplet evaporation rates. This section presents them.

8.1 The Effect of Ambient Pressure

Yoon and Baek⁴⁴ studied the effects of a high-pressure environment on the nanofuel droplet evaporation characteristics of Al–kerosene nanofuels. The conditions were the same as used by Javed et al.¹⁶, with oleic acid as the surfactant, but with an operating temperature range of 300–700 °C and variations in ambient pressure values of 0.1 and 2.5 MPa. The results indicated that at low temperature conditions, 300–600 °C, the evaporation rate of the nanofuel droplets with a nanoparticle concentration of 0.1 wt% decreased as the ambient pressure was increased, but at 700 °C the evaporation rate increased with increase in the ambient pressure. At a nanoparticle concentration of 1.0 wt%, this reversal was observed earlier at an operating temperature of 600 °C. The authors suggested that these phenomena were due to the contrasting effects of the heat of vaporization and diffusion coefficient of the nanofuel droplets. The earlier characteristic induces a faster evaporation rate when it is decreased (see Eq. 4), whilst the later reduces the evaporation rate when it decreases. At high pressure and temperature conditions, the decrease of the heat of vaporization becomes more dominant compared to the diffusion coefficient, therefore, the rate of evaporation of the nanofuel droplets increases.

8.2 The Effect of Surface Tension

Gerken et al.¹³ didn't report any changes in the surface tension of the Al–ethanol nanofuel droplets they studied even after increasing the PLR from 0 to 3 wt%. Their experiments were conducted under room temperature conditions (297 K) and 35–45% relative humidity with no forced convection. The author is not aware of any other study examining the effects of surface tension on the evaporation of nanofuels, however,

other scholars^{6, 20, 22, 40} observed changes in the surface tension values when NPs were dispersed in base fluids.

8.3 Other Conditions

The effects of the radiation levels (see Sect. 6.2.1), operating temperature (Sects. 3.2, 6.2.1, 6.2.2, 7, 8.1) and the types of base fuels (Sect. 5) are implicit in earlier sections.

9 Some Remarks and Possible Scope for Further Studies

Nanofuels present an exciting alternative to pure hydrocarbon fuels that can potentially reduce the emissions from internal combustion engines. Further studies are still required and a few areas are enumerated thus:

1. The effects of the stability of the nanofuel suspensions on the droplet evaporation mechanisms need further investigation. This is because the NPs can settle out of suspension well before the potential benefits of the additives can be used.
2. The effects of the thermo-physical properties (including viscosity, surface tension, etc.) of the NPs on the evaporation mechanisms of the nanofuel suspensions need further investigations. For example, what are the optimum time scales for the formation of the NP aggregates and for droplet micro-explosions? These are important because these can either increase the droplet evaporation rate or reduce it depending on when it forms. Pathak and Basu²⁹ have alluded to the dependence of the fuel droplet bubble-bursting events to the droplet lifetime in nanofuel bubble-boiling studies.
3. Following on from (2) above, the droplet nucleation and micro-explosion phenomena could be further explained using microscopic imaging studies. Similar studies have already been carried out for burning nanofuels³.
4. The types of surfactants, the concentration levels and their effects on the properties of the base fuel before the addition of the NPs need to be ascertained.
5. Other qualitative and quantitative mechanisms by which NPs influence the evaporation rates/phases of nanofuel suspensions need to be identified and clearly quantified.

6. The development of analytical, and numerical models for the nanofuel droplet evaporation processes would greatly aid the experimental processes as has happened for fuel droplet evaporation processes without additives^{36, 37}. Population balance equation models¹⁰ to understand the particle aggregation process, modelling of the optical properties using the Rayleigh approximation¹² and Monte Carlo methods⁴², and more sophisticated kinetic dynamics and molecular dynamics models³⁶ can all be explored.

The goal is to have optimum combinations of surfactants, NPs and the base fuel to replicate desired specific nanofuel droplet evaporation characteristics that can be used to better control the combustion and hence, emissions of ICEs using such fuels.

10 Conclusions

Nanofuels can be characterised as stable colloidal suspensions of nanoparticles in a base fuel, and they have potential applications in the combustion and propulsion sectors. From the available literature on the studies of nanofuel evaporation, it can be concluded that the precise effects of a NP additive on a base fuel depend on the relative strengths of interacting conditions such as the ambient temperature, pressure, and radiation levels, the PLR of the NP, the surfactant used and its loading, and the physical properties of the base fuel. These can vary widely depending on the conditions. We can conclude from the studies that:

1. Three distinct phases of the nanofuel droplet evaporation process have been identified: (1) the heat-up phase, (2) the steady-state phase, and, depending on the ambient conditions (3) a droplet dry-out phase or a droplet distortion/micro-explosion phase.
2. Depending on what the operating conditions are, the nanofuel droplet diameter may or may not diminish during the evaporation process following the D^2 law. The presence of NP agglomerates at high PLRs and at high-temperature environments leads to deviations from the D^2 law.
3. The ambient temperature conditions can promote nanofuel droplet evaporation rate increase by increasing the nanofuel droplet temperature through radiative absorption of the NP additives.

4. The rate of the nanofuel droplet evaporation, promoted by radiation absorption, depends on the type of NP additive and its rate of radiative energy absorption.
5. However, there is an optimum loading level for the NPs beyond which there is a retardation of the droplet rate of evaporation. This is due to the formation NP agglomerates on the droplet surface which inhibit the droplet evaporation.
6. There is an optimum loading level beyond which the surfactant can retard the evaporation rate of the nanofuel droplets by forming monolayers of itself over the fuel droplet, and or by forming droplet distortions due to the entrapment of its volatile components in the fuel droplet.
7. At the droplet dry-out phase, the fuel liquid in the nanofuel solution completely dries out, leaving NP agglomerates behind. These occur at relatively natural or weak forced convection conditions.
8. However, at high ambient temperatures, the NP agglomerates left on the surface of the fuel droplets after the evaporation of most of the fuel droplets during the steady-state phase are exposed to these high temperatures. They consequently heat up the remaining fuel liquid causing droplet distortions and micro-explosions.
9. If the ambient conditions are of temperature values higher than both the boiling point of the base fuel and the melting point of the metallic NPs, there would be simultaneous burning of the base fuel and the NP, with intense micro-explosions.

List of Symbols

Al: Aluminum; Al_2O_3 : Aluminum oxide; B : Transfer number; CNP: Carbon nanoparticles; D, d : Droplet diameter, m; D_0, d_0 : Initial droplet diameter, m; D_1 : Droplet diameter at the end of the heat-up phase, m; ICE: Internal combustion engine; K : Thermal conductivity, J/m s K; L : Latent heat of fuel vaporization, J/kg; MWCNT: Multiwalled carbon nanotubes; NP: Nanoparticle; P : Ambient pressure, kPa; PLR: Particle loading rate, wt%; T : Temperature, K; t : Time, s; wt%: Percentage by weight; c_p : Specific heat at constant pressure, J/kg K.

Greek Symbols

Δt_{hu} : Duration of the droplet evaporation heat-up period, s; Δt_{st} : Duration of the droplet evaporation steady-state period, s; μ : Dynamic viscosity,

kg/m s; λ : Evaporation constant, m^2/s ; λ_{hu} : Evaporation constant, m^2/s ; λ_{st} : Evaporation constant, m^2/s ; ρ : Density, kg/m^3 .

Subscripts

st: Droplet evaporation steady-state period; hu: Droplet evaporation heat-up period; 0: Initial value; s: Value at the fuel droplet surface; ∞ : Ambient value.

Acknowledgements

This work was supported by the University Grant Commission—UK India Education and Research Initiative CHAPNA project: UGC-UKIERI 2016-17-050.

Received: 19 July 2018 Accepted: 10 September 2018
Published online: 6 October 2018

References

1. Allen C, Lee T (2009) Energetic-nanoparticle enhanced combustion of liquid fuels in a rapid compression machine. In: 47th AIAA aerospace sciences meeting including the new horizons forum and aerospace exposition, p 227
2. Asibor J, Pandey K, Basu S, Emekwuru N (2018) Characterization of the spray cone angles of fuels with nanoparticle additives. In: ICLASS-2018, proceedings of the 14th triennial international conference on liquid atomization and spray systems
3. Basu S, Miglani A (2016) Combustion and heat transfer characteristics of nanofluid fuel droplets: a short review. *Int J Heat Mass Transf* 96:482–503
4. Bazyn T, Krier H, Glumac N (2006) Shock tube measurements of combustion of nano-aluminum. In: 44th AIAA aerospace sciences meeting and exhibit, p 1157
5. Chen RH, Phuoc TX, Martello D (2010) Effects of nanoparticles on nanofluid droplet evaporation. *Int J Heat Mass Transf* 53(19–20):3677–3682
6. Chen RH, Phuoc TX, Martello D (2011) Surface tension of evaporating nanofluid droplets. *Int J Heat Mass Transf* 54(11–12):2459–2466
7. DeLuca LT, Galfetti L, Severini F (2005) Combustion of composite solid propellants with nanosized aluminium. *Combust Explos Shock Waves* 41(6):680–692
8. Faeth GM (1979) Current status of droplet and liquid combustion. In: Chigier NA (ed) *Energy and combustion science*. Pergamon, Oxford, pp 149–182
9. Galfetti L, DeLuca LT, Severini F, Colombo G, Meda L, Marra G (2007) Pre and post-burning analysis of nano-aluminized solid rocket propellants. *Aerosp Sci Technol* 11(1):26–32
10. Gan Y, Qiao L (2011) Evaporation characteristics of fuel droplets with the addition of nanoparticles under

- natural and forced convections. *Int J Heat Mass Transf* 54(23–24):4913–4922
11. Gan Y, Qiao L (2012) Radiation-enhanced evaporation of ethanol fuel containing suspended metal nanoparticles. *Int J Heat Mass Transf* 55(21–22):5777–5782
 12. Gan Y, Qiao L (2012) Optical properties and radiation-enhanced evaporation of nanofluid fuels containing carbon-based nanostructures. *Energy Fuels* 26(7):4224–4230
 13. Gerken WJ, Thomas AV, Koratkar N, Oehlschlaeger MA (2014) Nanofluid pendant droplet evaporation: experiments and modeling. *Int J Heat Mass Transf* 74:263–268
 14. Godsave GAE (1953) Studies of the combustion of drops in a fuel spray—the burning of single drops of fuel. In: Symposium (international) on combustion, Elsevier, vol 4, no 1, pp 818–830
 15. Ivanov GV, Tepper F (1997) In: 4th International symposium on special topics in chemical propulsion, Begell House, New York, p 636
 16. Javed I, Baek SW, Waheed K, Ali G, Cho SO (2013) Evaporation characteristics of kerosene droplets with dilute concentrations of ligand-protected aluminum nanoparticles at elevated temperatures. *Combust Flame* 160(12):2955–2963
 17. Javed I, Baek SW, Waheed K (2013) Evaporation characteristics of heptane droplets with the addition of aluminum nanoparticles at elevated temperatures. *Combust Flame* 160(1):170–183
 18. Javed I, Baek SW, Waheed K (2014) Effects of dense concentrations of aluminum nanoparticles on the evaporation behavior of kerosene droplet at elevated temperatures: the phenomenon of microexplosion. *Exp Therm Fluid Sci* 56:33–44
 19. Johnson C, Parr T, Hanson-Parr D, Hollins R, Fallis S, Higa K (2000) Combustion and oxidation of metal nanoparticles and composite particles. In: Proceedings of the 37th JANNAF combustion subcommittee meetings
 20. Kannaiyan K, Sadr R (2017) The effects of alumina nanoparticles as fuel additives on the spray characteristics of gas-to-liquid jet fuels. *Exp Therm Fluid Sci* 87:93–103
 21. Karmakar S, Som SK, Rao DCK (2018) Combustion of multi-component fuel droplets. *Droplets and sprays*. Springer, Singapore, pp 77–114
 22. Khond VW, Kriplani VM (2016) Effect of nanofluid additives on performances and emissions of emulsified diesel and biodiesel fueled stationary CI engine: a comprehensive review. *Renew Sustain Energy Rev* 59:1338–1348
 23. Kuo KK, Luca LT (2002) Combustion of energetic materials. Begell House Publisher, Danbury
 24. Kuo KK, Risha GA, Evans BJ, Boyer E (2003) Potential usage of energetic nano-sized powders for combustion and rocket propulsion. In: MRS proceedings, vol 800. Cambridge University Press, p AA1.1
 25. Lefebvre AH, McDonnell VG (2017) Atomization and sprays. CRC Press, Boca Raton
 26. Mench MM, Kuo KK, Yeh CL, Lu YC (1998) Comparison of thermal behavior of regular and ultra-fine aluminum powders (Alex) made from plasma explosion process. *Combust Sci Technol* 135(1–6):269–292
 27. Miglani A, Basu S (2015) Effect of particle concentration on shape deformation and secondary atomization characteristics of a burning nanotitania dispersion droplet. *J Heat Transfer* 137(10):102001
 28. Pantoya ML, Granier JJ (2005) Combustion behavior of highly energetic thermites: nano versus micron composites. *Propellants Explos Pyrotech Int J Deal Sci Technol Asp Energ Mater* 30(1):53–62
 29. Pathak B, Basu S (2016) Phenomenology of break-up modes in contact free externally heated nanoparticle laden fuel droplets. *Phys Fluids* 28(12):123302
 30. Pivkina A, Ulyanova P, Frolov Y, Zavyalov S, Schoonman J (2004) Nanomaterials for heterogeneous combustion. *Propellants Explos Pyrotech Int J Deal Sci Technol Asp Energ Mater* 29(1):39–48
 31. Rai A, Park K, Zhou L, Zachariah MR (2006) Understanding the mechanism of aluminium nanoparticle oxidation. *Combust Theor Model* 10(5):843–859
 32. Reid DL, Russo AE, Carro RV, Stephens MA, LePage AR, Spalding TC, Petersen EL, Seal S (2007) Nanoscale additives tailor energetic materials. *Nano Lett* 7(7):2157–2161
 33. Risha GA, Boyer E, Evans B, Kuo KK, Malek R (2003) Characterization of nano-sized particles for propulsion applications. In: MRS proceedings, vol 800. Cambridge University Press, p AA6.6
 34. Rozenband VI, Vaganova NI (1992) A strength model of heterogeneous ignition of metal particles. *Combust Explos Shock Waves* 28(1):1–7
 35. Saxena V, Kumar N, Saxena VK (2017) A comprehensive review on combustion and stability aspects of metal nanoparticles and its additive effect on diesel and biodiesel fuelled CI engine. *Renew Sustain Energy Rev* 70:563–588
 36. Sazhin SS (2017) Modelling of fuel droplet heating and evaporation: recent results and unsolved problems. *Fuel* 196:69–101
 37. Sazhin SS, Rybdylova O, Pannala AS, Somavarapu S, Zaripov SK (2018) A new model for a drying droplet. *Int J Heat Mass Transf* 122:451–458
 38. Shaafi T, Sairam K, Gopinath A, Kumaresan G, Velraj R (2015) Effect of dispersion of various nanoadditives on the performance and emission characteristics of a CI engine fuelled with diesel, biodiesel and blends—a review. *Renew Sustain Energy Rev* 49:563–573
 39. Shin YJ, Shen YH (2007) Preparation of coal slurry with organic solvents. *Chemosphere* 68(2):389–393
 40. Tanvir S, Qiao L (2012) Surface tension of nanofluid-type fuels containing suspended nanomaterials. *Nanoscale Res Lett* 7(1):226
 41. Tanvir S, Qiao L (2016) Droplet burning rate enhancement of ethanol with the addition of graphite nanoparticles: influence of radiation absorption. *Combust Flame* 166:34–44
 42. Tanvir S, Biswas S, Qiao L (2017) Evaporation characteristics of ethanol droplets containing graphite

- nanoparticles under infrared radiation. *Int J Heat Mass Transf* 114:541–549
43. Tyagi H, Phelan PE, Prasher R, Peck R, Lee T, Pacheco JR, Arentzen P (2008) Increased hot-plate ignition probability for nanoparticle-laden diesel fuel. *Nano Lett* 8(5):1410–1416
44. Yoon J, Baek SW (2015) Droplet evaporation behavior of kerosene/nano-aluminum fuels at high pressure environment. *Int J Mater Mech Eng (IJMME)* 4:44–49



Dr. Emekwuru is interested in the fundamental studies of thermofluids systems, the development of more efficient numerical schemes for the characterization of these systems, and the development of experimental processes to validate the schemes. As an Ogden Trust PhD Teaching Fellow at the University of Manchester, he helped to develop a computational method

that enabled the representation of spray processes without expensively tracking the trajectories of groups of droplets. Since joining Coventry University in 2015, he has continued to work on the detailed understanding of thermofluids processes. Some of the results have been applied to increase the efficiency of internal combustion engines and solar thermal cooling/heating systems.